Supporting Information

Park et al. 10.1073/pnas.1218872110

SI Materials and Methods

Protein Extraction. Protein extracts for affinity chromatography were prepared as described (1) from the systemic (asymptomatic) leaves of Columbia (Col-0) *Arabidopsis*, challenged with spore suspensions of *Alternaria brassicicola* (15 μL droplets containing 1×10^7 spores per milliliter).

Flow-Through Jasmonic Acid Affinity Chromatography. The (-)-jasmonic acid (JA)-immobilized resin was prepared by using a PharmaLink Immobilization Kit (Pierce) according to the manufacturer's instructions; the coupling with 0.5 to 5 mg JA typically resulted in 150 to 250 μg JA-immobilized per milliliter resin. Following protein extract loading, the JA-affinity column was washed with loading buffer without and then with 10 mM cucurbic acid to remove nonspecifically bound proteins. Column-bound proteins were eluted with loading buffer containing 5 mM JA and 100 mM glycine buffer (pH 2.7) containing 500 mM NaCl. PharmaLink coupling resin without covalently bound JA (i.e., mock column) was used as control. Note that loading buffer consisted of 50 mM KPO_4 (pH 7.0), 50 mM NaCl, a protease inhibitor mixture (Sigma), and detergent (0–0.5%, vol/vol). The separations presented in Fig. 1*A* and Fig. S2 were carried out with 0.1% (vol/vol) Triton X-100.

Preparation of Arabidopside G. Arabidopside G, 1,2-di-*O*-(12-oxophytodienoyl)-3-*O*-(6′-*O*-(12-oxo-phytodienoyl)-β-*D*-galactopyranosyl)-sn-glycerol, was prepared from a lipid extract obtained from 200 g of 6-wk-old *Arabidopsis* rosettes 30 min after freeze/thawing as this induces arabidopside formation (2–4).

Pathogen Infections and Quantification of Disease Severity. Infection analyses with *Pseudomonas syringae (Pst* DC3000) were carried out by using syringe infiltration (5). Infection analyses with *A. brassicicola* (ATCC 96866; American Type Culture Collection) were carried out by challenge with spore suspensions (6).

Quantification of JA and (+)-12-oxo-Phytodienoic Acid. The samples of JA [(1*R*,2*R*)-3-oxo-2-(2*Z*)-2-pentenyl-cyclopentaneacetic acid] and (+)-12-oxo-phytodienoic acid [OPDA; (1*S*,2*S*)-3-oxo-2-(2*Z*-pentenyl)-cyclopent-4-ene-1-octanoic acid] were prepared from leaves, harvested at 0 and 3 h after wounding or OPDA treatment (7). The jasmonates were separated by HPLC equipped with a reversed-phased column (C18 Luna 5.0 μm, 150 × 2.1 mm; Phenomenex) by using a binary solvent system composed of water with 0.1% (vol/vol) HCOOH and MeOH with 0.1% HCOOH as a mobile phase at a flow rate of 0.2 mL/min. Separations were performed stepwise: 30% methanol for 4 min, 60% for 6 min, linear increase to 95% for 12.5 min. Identity of jasmonates was confirmed by ion fragmentation on a triple-stage quadrupole mass spectrometer (Thermo Finnigan) with direct injection and operated with a source voltage of 4.0 kV and source temperature of 300 °C. The analysis parameters were optimized by teeing 10 ng/μL of standard compound, (-)-dihydrojasmonic acid [HJA; 2-((1*R*,2*R*)-3-oxo-2-pentylcyclopentyl)acetic acid], JA, and OPDA in 50% MeOH with 0.1% HCOOH at a flow rate of 0.2 mL/min, in multiple reaction-monitoring mode; the fragments *m/z* 211.20 → 193.10 (JA), 213.20 → 195.1 (HJA) and 293.4 → 275.4 (OPDA) were monitored in a positive mode and used for the quantification, respectively.

Quantitative RT-PCR. Total leaf RNA was prepared using TRIzol reagent (Invitrogen) and RNase-free DNase (RQ1; Promega) according to the manufacturer's instructions. RNA qualities were assessed by agarose gel electrophoresis and NanoDrop ($A_{260}/A_{280} > 1.8$ and $A_{260}/A_{230} > 2.0$) (8). RT reactions were performed by using an oligo(dT) reverse primer and a reverse transcriptase (SuperscriptII; Invitrogen). The cDNA were assessed by quantitative PCR with two sets of housekeeping genes, *POLYUBIQUITIN* (*UBC*) and *GAPDH* (9). Quantitative PCR was performed with the SensiMix SYBR and Fluorescein kit (Bioline) in an iCycler iQ5 (Bio-Rad) PCR system cycled 40 times by using gene-specific primer sets (Table S2). The annealing temperatures for the primer pairs were 60 °C [*THIONIN 2.1* (*THI2.1*), *VEGETATIVE STORAGE PROTEIN 2* (*VSP2*) and *UBC*] and 53 °C [*GLUTAREDOXIN 480* (*GRX480*), *CYTOCHROME P450* (*CYP81D11*), *GLUTATHIONE S-TRANSFERASE 6* (*GST6*), *GST8, HEAT SHOCK PROTEIN 17.6* (*HSP17.6*), *GLUTATHONE REDUCTASE 1* (*GR1*), *GR2, UBC* and *GAPDH*]. To determine the relative abundance of target transcripts, the average threshold cycle (i.e., Ct) was normalized to that of *UBC* as $2^{-\Delta Ct}$, where $-\Delta Ct = (C_{t,gene} - C_{t,UBC})$.

Semiquantitative RT-RCR. A total of 2 μL of cDNA prepared as described earlier was used for semiquantitative RT-PCR, performed with GoTaq Green master mix (Promega). The annealing temperature for primer pairs was 55 °C. The PCR profiles were 40 cycles [*OPDA REDUCTASE 3* (*OPR3*)], 30 cycles [*PLANT DEFENSIN 1.2* (*PDF1.2*), *CYCLOPHILIN 20-3* (*CYP20-3*), *SERINE ACETYLTRANSFERASE 1* (*SAT1*), *O-ACETYLSERINE (THIOL)LYASE B* (*OASTL-B*) and *CYP20-2*] or 25 cycles (*UBC* and *ACTIN*). Each cycle consisted of 94 °C for 30 s, annealing temperature for 30 s, and 72 °C for 1 min; the final step occurred at 72 °C for 10 min.

Microscopy Imaging and Ratiometric Analysis. Plants expressing *redox-sensitive GFP2* (*roGFP2*) were placed on a slide in a drop of double-distilled H_2O and imaged as described previously (10) by using a Nikon Eclipse TE2000-U inverted microscope with a swept field confocal system (Prairie Tech) equipped with lasers for 405/488 nm excitation and excitation filter (ET535/50) for emission light. Ratiometric analysis of fluorescence images was performed after background subtraction in ImageJ (http://rsb.info.nih.gov/ij/) as previously described (10).

1. Park S-W, Lawrence CB, Linden JC, Vivanco JM (2002) Isolation and characterization of a novel ribosome-inactivating protein from root cultures of pokeweed and its mechanism of secretion from roots. *Plant Physiol* 130(1):164–178.
2. Andersson MX, et al. (2006) Oxylipin profiling of the hypersensitive response in Arabidopsis thaliana. Formation of a novel oxo-phytodienoic acid-containing galactolipid, arabidopside E. *J Biol Chem* 281(42):31528–31537.
3. Kourtchenko O, et al. (2007) Oxo-phytodienoic acid-containing galactolipids in *Arabidopsis*: Jasmonate signaling dependence. *Plant Physiol* 145(4):1658–1669.
4. Nilsson AK, Fahlberg P, Ellerström M, Andersson MX (2012) Oxo-phytodienoic acid (OPDA) is formed on fatty acids esterified to galactolipids after tissue disruption in *Arabidopsis thaliana*. *FEBS Lett* 586(16):2483–2487.
5. Liu J, et al. (2009) RIN4 functions with plasma membrane H^+-ATPases to regulate stomatal apertures during pathogen attack. *PLoS Biol* 7(6):e1000139.
6. van Wees SC, Chang HS, Zhu T, Glasebrook J (2003) Characterization of the early response of *Arabidopsis* to *Alternaria brassicicola* infection using expression profiling. *Plant Physiol* 32:606–617.
7. Pan X, Welti R, Wang X (2008) Simultaneous quantification of major phytohormones and related compounds in crude plant extracts by liquid chromatography-electrospray tandem mass spectrometry. *Phytochemistry* 69(8):1773–1781.
8. Udvardi MK, Czechowski T, Scheible W-R (2008) Eleven golden rules of quantitative RT-PCR. *Plant Cell* 20(7):1736–1737.
9. Czechowski T, Stitt M, Altmann T, Udvardi MK, Scheible WR (2005) Genome-wide identification and testing of superior reference genes for transcript normalization in *Arabidopsis*. *Plant Physiol* 139(1):5–17.
10. Meyer AJ, et al. (2007) Redox-sensitive GFP in *Arabidopsis thaliana* is a quantitative biosensor for the redox potential of the cellular glutathione redox buffer. *Plant J* 52(5):973–986.

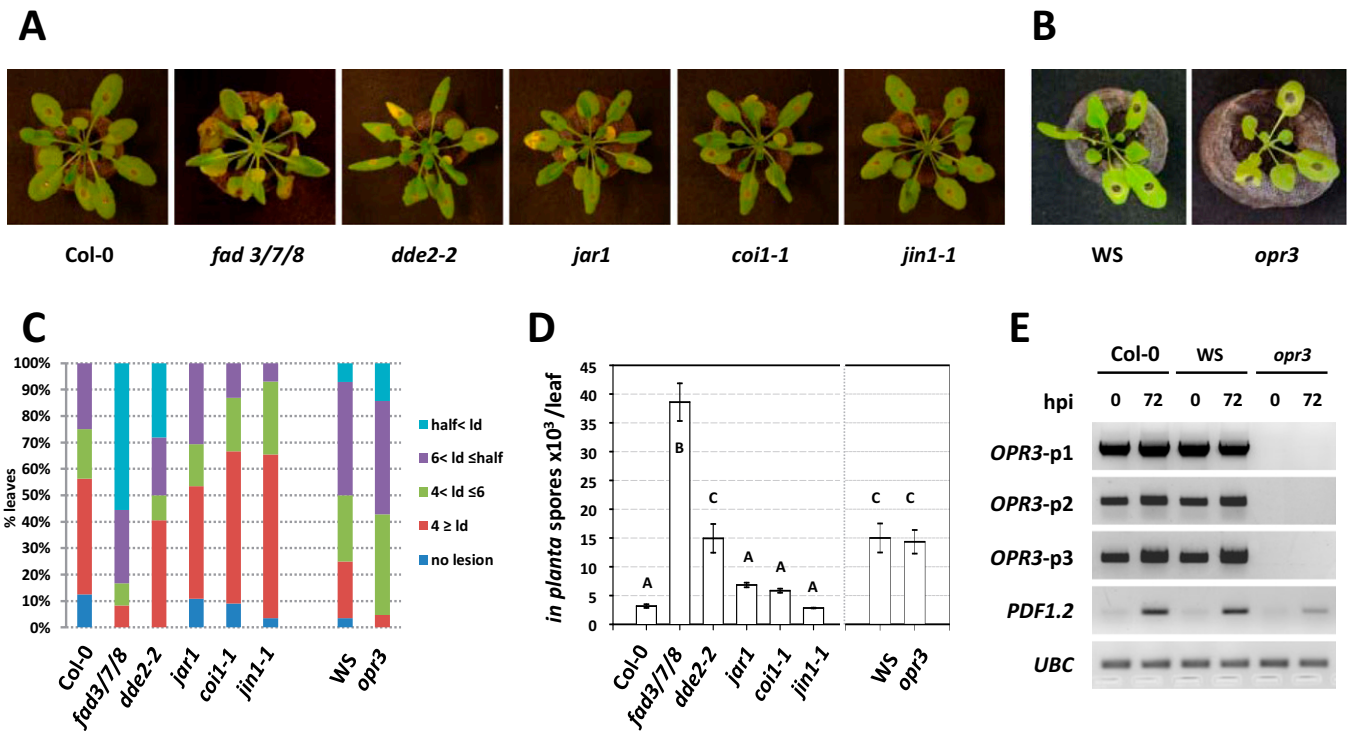

Fig. S1. Quantification of disease severity in *Arabidopsis* mutants challenged with *A. brassicicola*. (*A* and *B*) Lesion development. (*C*) Distribution of disease severity classes. Disease severity was expressed as the percentage of leaves falling in the following disease severity classes: no lesion, 4 ≥ lesion diameter (ld), 4 < ld ≤ 6, 6 < ld ≤ half, or half < ld (no lesion development, ld < 4 mm, between 4 and 6 mm, between 6 mm and the half of leaf area, or expanding over the half of leaf), respectively. Data represent results from 30 to 40 leaves of 12 plants per genotype. (*D*) Average number of *in planta*-formed spores per leaf ± SD. Each data point is the average of three pools of 16 inoculated leaves of four plants per genotype. Different letters indicate statistically significant differences between genotypes [Tukey–Kramer honestly significant difference (HSD) test on all pairs; $\alpha = 0.05$]. In *A–D*, photographs and measurements were taken at 5 d (Col-0 ecotype background) and 3 d [Wassilewskija ecotype background] after application of 10-μL droplets containing 1×10^6 spores per milliliter on ~2 mo-old plants. (*E*) *opr3* is a loss-of-function mutant. Semiquantitative RT-PCR analyses of *OPR3* in *A. brassicicola* inoculated WT (Columbia and Wassilewskija) and *opr3* mutant plants. Total RNAs were prepared from the leaves of each plant, harvested at 0 and 72 hpi. Three sets of *OPR3*-specific primers (*OPR3*_p1-p3 in Table S2), including the one used by Chehab et al (1), were used to avoid a false detection. The PCR reactions were carried out for 40 cycles (*OPR3*), 30 cycles (*PDF1.2*) (2), or 25 cycles (*UBC*), respectively. The transcript levels of *UBC* (3) were used as an equal loading control.

1. Chehab EW, et al. (2011) Intronic T-DNA insertion renders *Arabidopsis opr3* a conditional jasmonic acid-producing mutant. *Plant Physiol* 156(2):770–778.
2. Stintzi A, Weber H, Reymond P, Browse J, Farmer EE (2001) Plant defense in the absence of jasmonic acid: The role of cyclopentenones. *Proc Natl Acad Sci USA* 98(22):12837–12842.
3. Czechowski T, Stitt M, Altmann T, Udvardi MK, Scheible WR (2005) Genome-wide identification and testing of superior reference genes for transcript normalization in *Arabidopsis*. *Plant Physiol* 139(1):5–17.

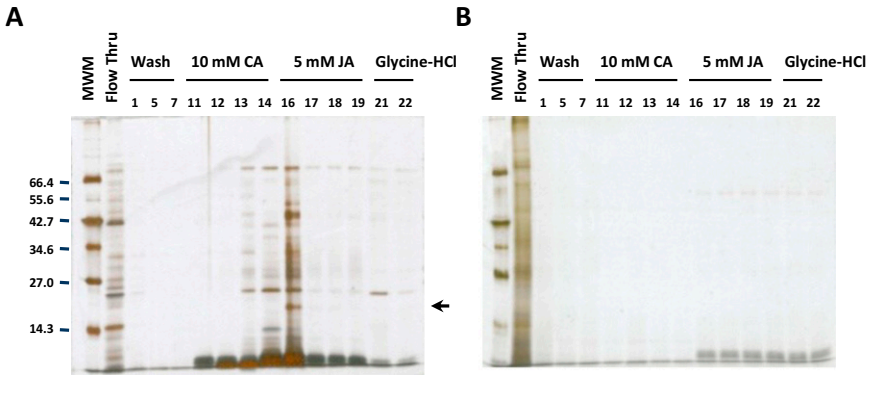

C

gi|461899 Mass: 28208 Score: 223 matched: 4 **emPAI:** 0.46
PREDICTED: Peptidyl-prolyl cis-trans isomerase CYP20-3, chloroplast
Sequence Coverage: **17%**

Matched peptides shown in **Bold Red**

1 MASSSSMQMV HTSRSIAQIG FGVKSQLVSA NRTTQSVCFG ARSSGIALSS
51 RLHYASPIK**Q FSGVYATTK**H QRTACVKSMA AEEEEVIEPQ AKVTNKVYFD
101 VEIGGEVAGR **IVMGLFGEVV PK**TVENFRAL CTGEKKYGYK GSSFHRIIKD
151 FMIQGGDFTE GNGT**GGISIY GAK**FEDENFT LKHTGPGILS MANAGPNTNG
201 SQFFICTVKT SWLDNKHVVF GQVIEGMKLV RTL**ESQETRA FDVPK**KGCRI
251 YACGELPLDA

Fig. S2. Affinity purification of putative jasmonate binding proteins (JBPs) from *Arabidopsis*. (*A*) Total protein extracts, prepared from the systemic leaves of *A. brassicicola*-infected *Arabidopsis*, were chromatographed on PharmaLink columns with covalently attached JA. After washing by using loading buffer without and then with 10 mM cucurbic acid, the column-retained proteins were eluted with loading buffer supplemented with 5 mM JA. A total of 12 μL of each 1.5-mL fraction was fractionated by SDS/PAGE, and the gel was silver-stained. (*B*) As a negative control, the same protein amount was fractionated on a matrix column that did not contain covalently bound JA, and parallel fractions were analyzed by SDS/PAGE. Very few protein bands could be detected in the JA eluate, even after extensive silver staining. Glycine-HCl buffer [0.1 M (pH 2.7), containing 0.5 M NaCl] was used to clean up the columns, and the fraction numbers are indicated above the lanes. The pools of fractions (e.g., no. 12–14, no. 16–18, and no. 21–22) were concentrated and subjected to MS analyses (electrospray ionization MS/MS) after trypsin digestion. MS analyses identified that JA eluate (e.g., fractions 16–18 in *A*) uniquely contains cyclophilin 20-3 (CYP20-3), comparing with fractions no. 12–14 and no. 21–22 (arrow indicates putative CYP20-3). Flow Thru, flow-through fraction; MWM, molecular weight of marker. (*C*) Mascot search engine (Matrix Science) compared MS-determined sequence of tryptic peptides with *Arabidopsis* database, and identified a putative JBP as CYP20-3. A protein of ~20 kDa enriched by JA-affinity chromatography (e.g., arrow in Fig. 1*A*) was carefully excised and subjected to MS analyses after trypsin digestion.

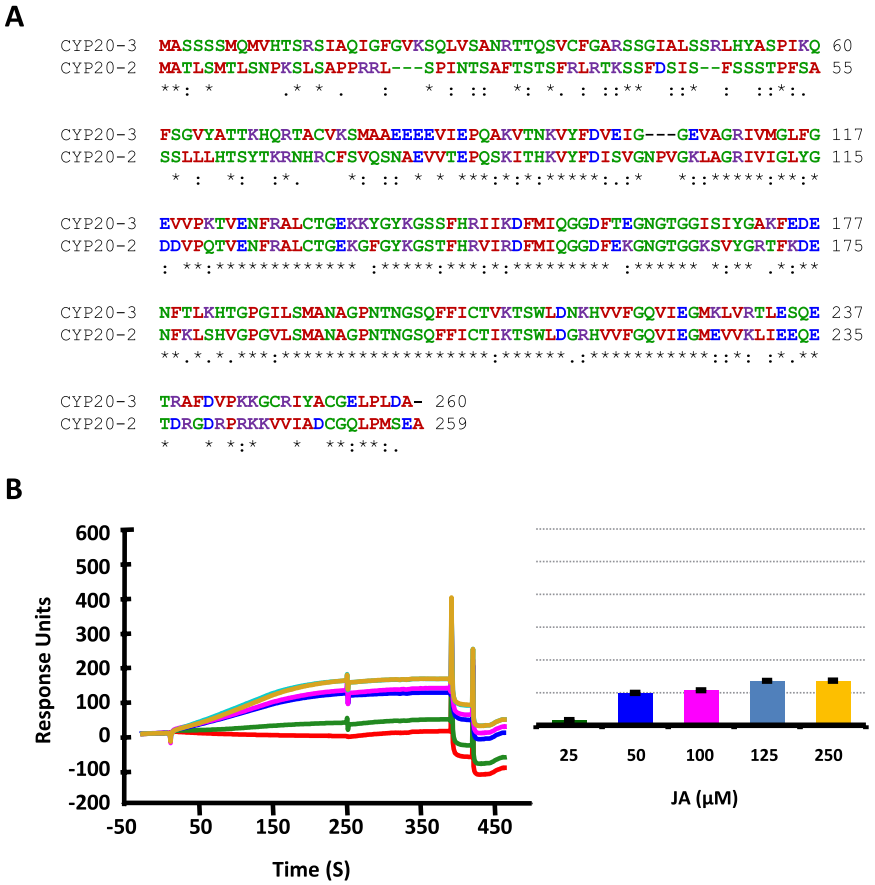

Fig. S3. CYP20-2, the thylakoid lumen localized homologue of CYP20-3, is not a JBP candidate. (*A*) Amino acid sequence alignment between CYP20-3 and CYP20-2 performed by ClustalW2 (1) (50% sequence identity at amino acid level). (*B*) SPR analyses of interaction between JA and CYP20-2. Final sensorgrams were obtained after subtraction of background values, buffer blank in flow cell, from raw interaction data.

1. Larkin MA, et al. (2007) Clustal W and Clustal X version 2.0. *Bioinformatics* 23(21):2947–2948.

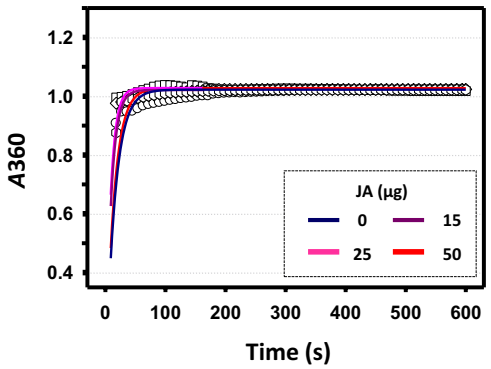

Fig. S4. JA displays no effect on the peptidyl-prolyl *cis-trans* isomerase (PPIase) activity of CYP20-3. The PPIase activity was determined by measuring the catalytic rate of the prolyl *cis*→*trans* interconversion of *cis* Succinyl-Ala-Leu-Pro-Phe-*para*-nitroanilide as previously described (1). Briefly, the assay was performed at 10 °C in 35 mM Hepes (pH 7.9), 0.015% (vol/vol) Triton X-100, 60 μM *cis*-peptide [dissolved in 60% (vol/vol) DMSO], and 250 μg/mL α-chymotrypsin, with CYP20-3. The reaction mixture was incubated at 10 °C until the absorbance baseline stabilized at 390 nm, and the reaction was initiated by the addition of α-chymotrypsin; absorbance was read every second. For the dependence of PPIase activity on JA, CYP20-3 was preincubated at 10 °C in the presence of varying concentrations of JA (15, 25, and 50 μg), and the remaining PPIase activity was determined.

1. Fischer G, Wittmann-Liebold B, Lang K, Kiefhaber T, Schmid FX (1989) Cyclophilin and peptidyl-prolyl cis-trans isomerase are probably identical proteins. *Nature* 337(6206):476–478.

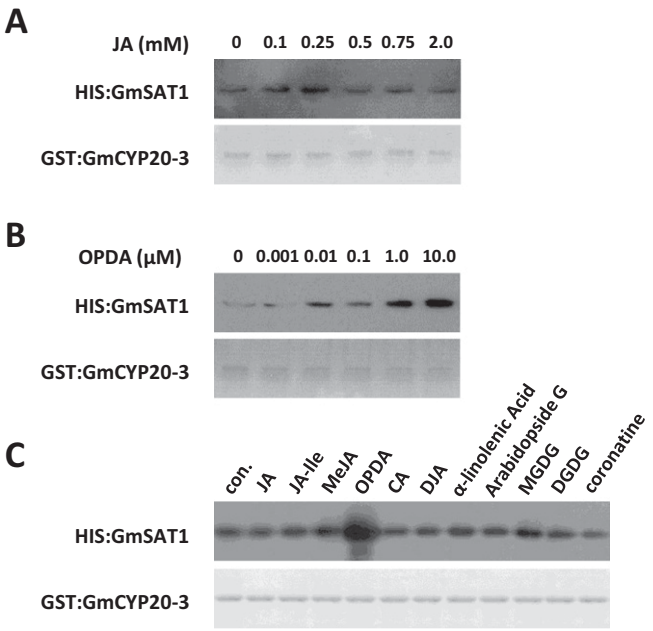

Fig. S5. OPDA promotes complex formation between *Glycine max* L. (Gm) CYP20-3 and Gm serine acetyltransferase 1 (SAT1). In vitro pull-down assays between GmCYP20-3 and GmSAT1 in the presence of various concentrations of JA (*A*), OPDA (*B*), or a broader effector screening with 500 μM of jasmonates and trienoic fatty acids (*C*). GST:GmCYP20-3 was used as a bait to pull down HIS:GmSAT1. (*Lower*) Coomassie blue-stained gels indicating the amount of bait protein used in each pull-down assay. Parallel immunoblots for proteins that copurified with GST:GmCYP20-3 were probed with monoclonal anti-His antibody (*Upper*). con., control; DGDG, digalactosyldiacylglycerol; MGDG, monogalactosyldiacylglycerol.

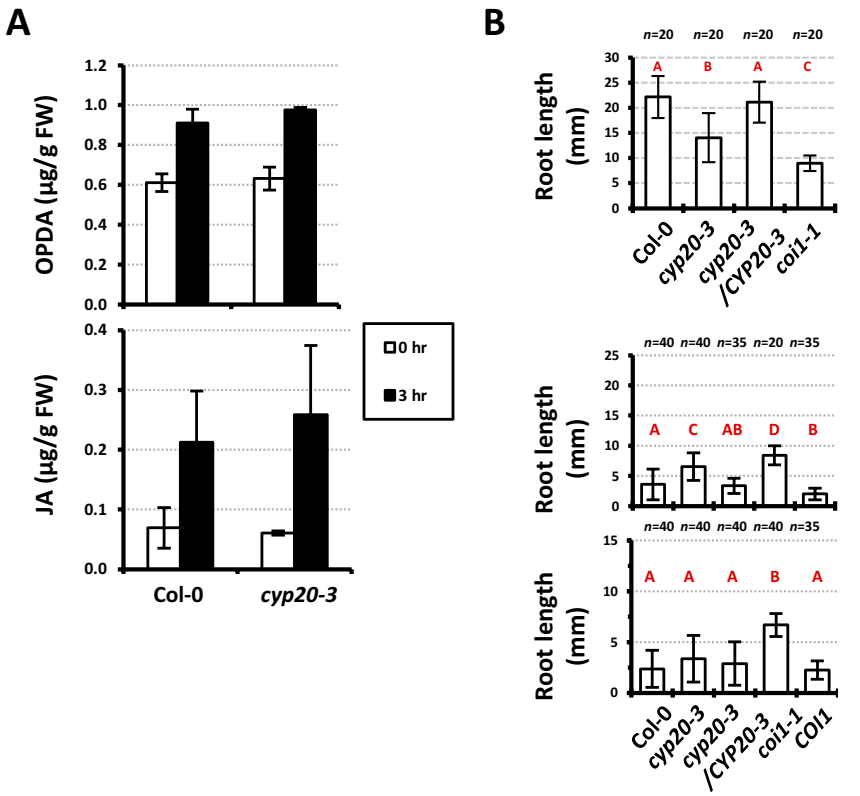

Fig. S6. *cyp20-3* plants showed insensitivity toward OPDA-mediated, but not JA-mediated, root growth inhibition, which is antagonized by the high light-induced root growth inhibition. (*A*) Levels of OPDA and JA, measured in Col-0 and *cyp20-3* plants after spraying OPDA (75 μM) on the leaf surface. Plants were germinated and grown at normal light intensity (80–100 μE/m^2/s) for ~1 mo before OPDA treatment, and jasmonates were extracted at 0 h (white bars) and 3 h (black bars) after OPDA treatment (data are mean ± SD, n = 3). The results confirmed that OPDA insensitivity of *cyp20-3* (Fig. 2*B*) is not associated with JA-mediated root growth inhibition. *cyp20-3* was capable of converting OPDA to JA like WT; therefore, the OPDA insensitivity of root growth in *cyp20-3* was independent of JA. (*B*) Root lengths at high light intensity (>200 μE/m^2/s) of Col-0 and mutant [*cyp20-3*, *cyp20-3*/*CYP20-3*, *coi1-1*, and *COI1* (*COI1*/*coi1*)] *Arabidopsis* plants in the absence and presence of OPDA (data are mean ± SD for n shown). Different letters indicate statistically significant differences between genotypes (Tukey–Kramer HSD test on all pairs; α = 0.05).

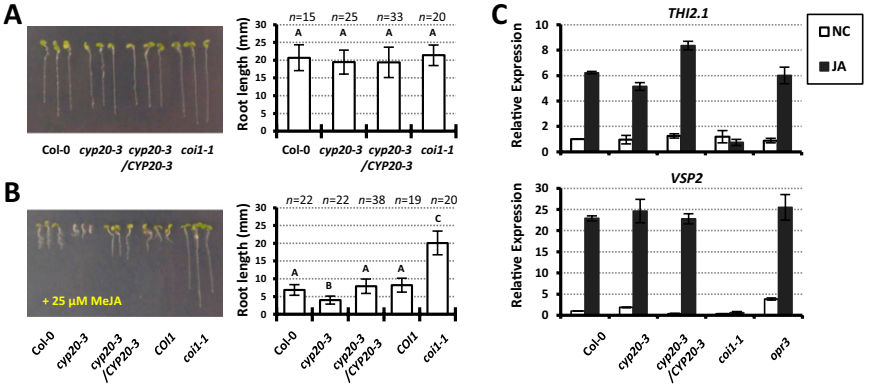

Fig. S7. CYP20-3 is not involved in JA-responsive signaling pathway. (*A* and *B*) Root growth analyses of Col-0 and mutant [*cyp20-3*, *cyp20-3*/*CYP20-3*, *coi1-1*, and *COI1* (*COI1*/*coi1*)] *Arabidopsis* plants in the absence (*A*) and presence (*B*) of 25 μM of methyl (+)-7-*iso*-jasmonate (MeJA; data are mean ± SD for n as indicated). Different letters indicate statistically significant differences between genotypes (Tukey–Kramer HSD test on all pairs; α = 0.05). (*C*) Quantitative RT-PCR analyses of JA-responsive genes (*THI2.1* and *VSP2*) (1) in JA-untreated (NC; white bars) and JA-treated (JA; black bars) Col-0 and mutant (*cyp20-3*, *cyp20-3*/*CYP20-3*, *coi1-1*, and *opr3*) *Arabidopsis* plants. Values were normalized to the expression levels of a housekeeping gene, *UBC* (2) (mean ± SD; n = 3).

1. Taki N, et al. (2005) 12-oxo-phytodienoic acid triggers expression of a distinct set of genes and plays a role in wound-induced gene expression in *Arabidopsis*. *Plant Physiol* 139(3): 1268–1283.
2. Czechowski T, Stitt M, Altmann T, Udvardi MK, Scheible WR (2005) Genome-wide identification and testing of superior reference genes for transcript normalization in *Arabidopsis*. *Plant Physiol* 139(1):5–17.

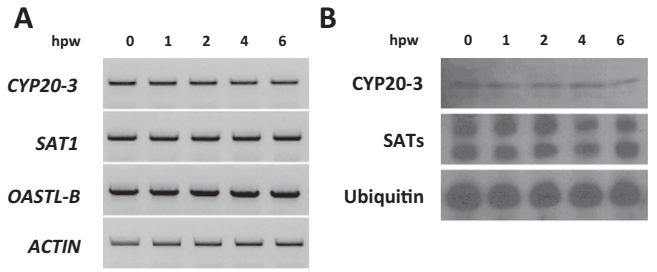

Fig. S8. Constitutive expressions of *CYP20-3*, *SAT1*, and *OASTL-B* during wound responses in WT (Col-0) *Arabidopsis*. (*A*) Time-resolved semiquantitative RT-PCR analyses of *CYP20-3*, *SAT1*, and *OASTL-B* in wounded Col-0 plants. Transcript levels of *ACTIN* were used as an equal loading control. (*B*) Time-resolved immunoblot analyses of CYP20-3 and serine acetyltransferases (SATs) in wounded Col-0 plants. For SATs, three isoforms [SAT1 (34.3 kDa), SAT2 (At2g17640, 42.7 kDa), SAT3 (At3g1310, 34.5 kDa)] were concomitantly detected by polyclonal anti-SAT antibody (1). The level of ubiquitin protein was used as an equal loading control.

1. Na G, Salt DE (2011) Differential regulation of serine acetyltransferase is involved in nickel hyperaccumulation in *Thlaspi goesingense*. *J Biol Chem* 286(47):40423–40432.

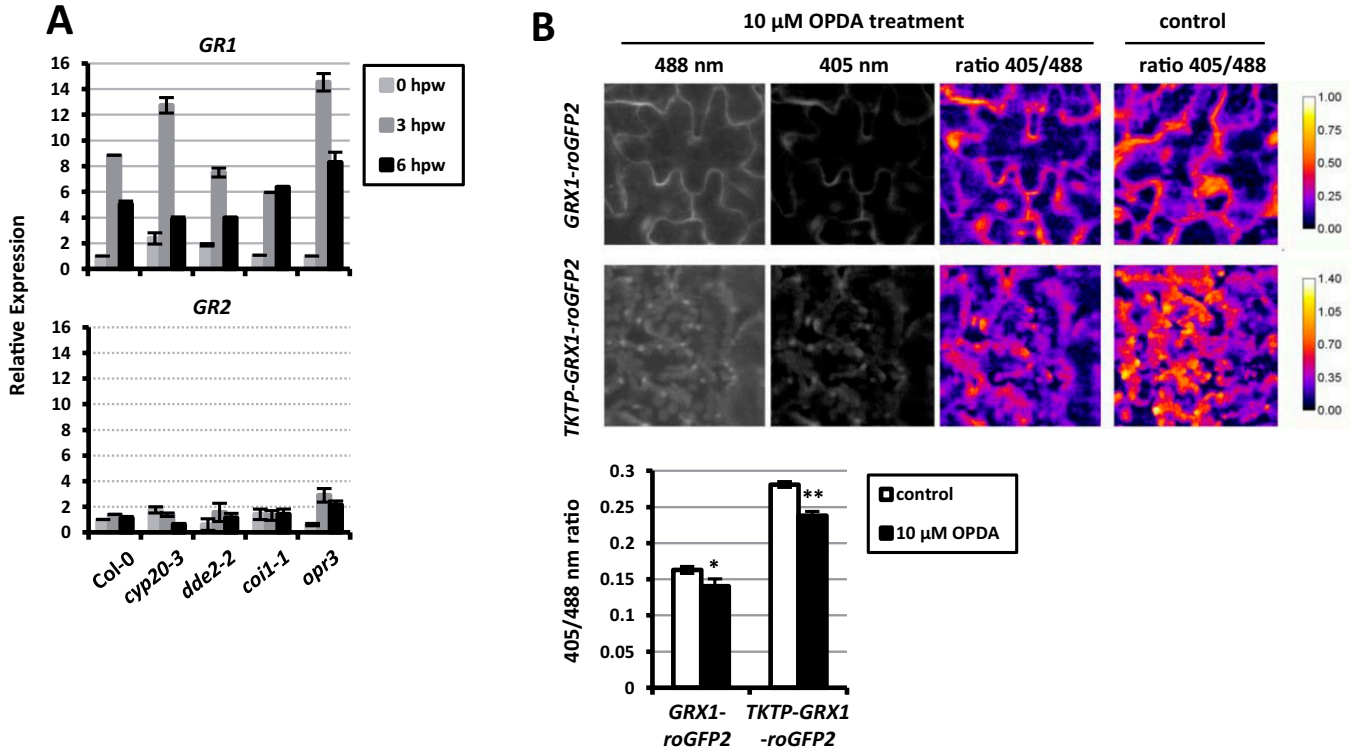

Fig. S9. Activity of GLUTATHIONE REDUCTASE 1 (GR1) has a minimal effect in wound-induced glutathione (GSH) accumulation, and exogenous OPDA treatment leads to enhanced reduction states of plastids and cytoplasm. (*A*) Transcript level regulation of *GR1* and *2* in wounded Col-0 and mutant (*cyp20-3*, *dde2-2*, *coi1-1*, and *opr3*) *Arabidopsis* plants. Time-resolved quantitative RT-PCR was performed with total RNAs, prepared from the leaves [harvested at 0, 3, and 6 h postwounding (hpw)] of each genotype. Values were normalized to the expression levels of a housekeeping gene, *UBC* (1) (mean ± SD, $n = 3$). Note that the increased GSH levels (e.g., Fig. 4*B*) could be caused by sulfur assimilation, protein degradation, or glutathione disulfide (GSSG) reduction (2, 3). Two genes encode GR, reducing GSSG to GSH, in *Arabidopsis*: cytosolic *GR1* and plastidic/mitochondrial *GR2* (4, 5). To tentatively investigate whether the GSSG reduction is involved in the wound-responsive regulation of redox homeostasis, the transcript levels of *GR*s were assessed in response to wounding. The levels of *GR1* (but not *GR2*) transcript were up-regulated in all tested genotypes. Despite the same transcriptional regulation of *GR1*, the wound-responsive GSH/thiol increases were high in WT but residual in *cyp20-3* and *dde2-2* (Fig. 4 *A* and *B*), suggesting that the contribution of GR activity in the wound-responsive buildup of reduction potential is negligible. (*B*) Redox-dependent fluorescent signals of redox-sensitive GFP2 in the cytosol (*GRX1-roGFP2*) and plastid (*TKTP-GRX1-roGFP2*) of *Arabidopsis* (6) were visualized at 30 min after OPDA treatment by confocal laser scanning microscopy with excitation at 405 and 488 nm (*Upper*) and ratiometric quantification of fluorescence emission. The color scale for the ratio values indicates reduced roGFP2 in blue and oxidized roGFP2 in yellow. Overall ratio values for the images were quantified (*Lower*; mean ± SD, $n \geq 9$). Different symbols indicate statistically significant differences between control and OPDA-treatment (Tukey–Kramer HSD test on all pairs; $\alpha = 0.05$). To tentatively assess whether OPDA-induced GSH/thiol production contributes to the changes in cellular redox homeostasis, redox-dependent modifications in the excitation efficiency of roGFP2 were determined and analyzed upon OPDA treatment. The enhanced reduction of roGFP2 in cytosol and plastids after OPDA application is reflected by the decrease in the 405/488-nm excitation ratio.

1. Czechowski T, Stitt M, Altmann T, Udvardi MK, Scheible WR (2005) Genome-wide identification and testing of superior reference genes for transcript normalization in *Arabidopsis*. *Plant Physiol* 139(1):5–17.
2. Leustek T, Martin MN, Bick JA, Davies JP (2000) Pathways and regulation of sulfur metabolism revealed through molecular and genetic studies. *Annu Rev Plant Physiol Plant Mol Biol* 51:141–165.
3. Meister A, Anderson ME (1983) Glutathione. *Annu Rev Biochem* 52:711–760.
4. Creissen G, Reynolds H, Xue YB, Mullineaux P (1995) Simultaneous targeting of pea glutathione reductase and of a bacterial fusion protein to chloroplast and mitochondria. *Plant J* 8:167–175.
5. Kaur N, Reumann S, Hu J (2009) Peroxisome biogenesis and function. *The Arabidopsis Book*, eds Somerville CR, Meyerowitz EM (American Society of Plant Biologists, Rockville, MD), pp 1–41.
6. Meyer AJ, et al. (2007) Redox-sensitive GFP in *Arabidopsis thaliana* is a quantitative biosensor for the redox potential of the cellular glutathione redox buffer. *Plant J* 52(5):973–986.

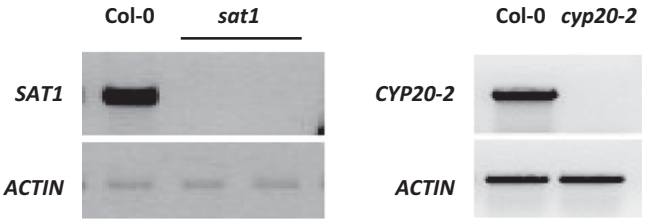

Fig. S10. Semiquantitative RT-PCR analysis confirmed the absence of *SAT1* and *CYP20-2* transcripts in corresponding mutant lines. Transcript levels of *ACTIN* were used as quantification control.

Table S1. Oligonucleotides used to identify homozygous KO mutants

Primer name	Target	Sequence (5′-3′)
p440-LP	*SAT1* left genomic primer	TGG CTA ATG ACC CTT AGA TAT GTG
p440-RP	*SAT1* right genomic primer	AGC TCC AAT CAA CAC ACC ATC
p971-LP	*CYP20-2* left genomic primer	TCA CCT ACC ATT TTT GCC AAC
p971-RP	*CYP20-2* right genomic primer	ACA GCT AGT TGC ATA CCC ACG
pLBb1.3	T-DNA specific primer	ATT TTG CCG ATT TCG GAA C

Table S2. Oligonucleotides used for RT-PCR

Gene	Direction	Sequence (5′-3′)
CYP20-3	Forward	TAA GTC GCA ATT AGT TTC
At3g62030	Reverse	CTA ACC ATG AAG T^CT TG
SAT1	Forward	CCC AAA TCG AAG ATG ACG AT
At1g55920	Reverse	CAC ACC ATC ACC AAT CTT CG
OASTL-B	Forward	GCT TTC GAT GTT TCC TCA GC
At2g43750	Reverse	GAA CAC A^AC GGC TAT GAG
CYP20-2	Forward	GAT GAC TCT GTC AAA
At5g13120	Reverse	CGG TCT CCT CTG TCT
ACTIN	Forward	TGC GAC AAT GGA ACT GGA ATG
At2g37620	Reverse	CTG TCT CGA GTT CCT GCT CG
CYP81D11	Forward	TCT CAA CAT G^GG TTT GTG AA
At3g28740	Reverse	AAG TAT C^AT AAC AAG TAT GA
HSP17.6	Forward	CTT GCC TGG ATT GAA GAA GG
At2g29500	Reverse	CAT CGC AGC CTT AAC CTG AT
GST8	Forward	TGA CAA GAA GCT G^TA TGA TGC
At1g78380	Reverse	ACA TAG CCA AAG TCA TCG CC
GRX480	Forward	TGA TTG TGA TTG GAC GGA GA
At1g28480	Reverse	TAA ACC GCC GGT AAC TTC AC
GST6	Forward	TGC CCT CAA C^CC CTT CGG TC
At2g47730	Reverse	GGT TGC CTT GAC TTT CTT GC
THI2.1	Forward	CT^C AGC TGA TGC TAC CAA TGA GC
At1g72260	Reverse	GCT CCA TTC ACA ATT TCA CTT GC
VSP2	Forward	CCT AAA GAA CGA CAC CGT CA
At5g24770	Reverse	TAC GG^A ACA GAG AAG ACC GA
PDF1.2	Forward	GCT GCT TTC G^AC GCA CCG GC
At5g44420	Reverse	TTA ACA TGG GAC GTA ACA GAT AC
*OPR3*_p1	Forward	CAC ATG ACG GCG GCA CAA GG
At2g06050	Reverse	TCA GAG GCG GGA AAA AGG A
*OPR3*_p2	Forward	TCT CTC ATC G^AG TGG TTC TG
At2g06050	Reverse	ACA TGT GGG AAC CCT GCG GA
*OPR3*_p3	Forward	CGG CGT TGG CAG AGT ATT AT
At2g06050	Reverse	TCC CTT AGC GTG AAC TGC TT
GR1	Forward	TTT TGC G^AA CAC TGC TTT TG
At3g24170	Reverse	AGC CTG AGG TGA AGA CCA GA
GR2	Forward	AAG GCA AAA GAA GGT GCT GA
At3g54660	Reverse	CCC TAA GTT^ CTT TGT GTT G
UBC	Forward	CTG CGA CTC AG^G GAA TCT TCT AA
At5g25760	Reverse	TTG TGC CAT TGA ATT GAA CCC
GAPDH	Forward	TTG GTG ACA ACA G^GT CAA GCA
At1g13440	Reverse	AAA CTT GTC GCT CAA TGC AAT C

The "^" symbol indicates the position of an exon–exon junction.